Kinetic Analysis of the Multivalent Ligand Binding Interaction between Protein A/G and IgG: a Standard System Setting

Peter P. Reader and Andrew M. Shaw*

University of Exeter Medical School, University of Exeter College of Life and Environmental Sciences,

Corresponding author:

Professor Andrew Shaw, University of Exeter, Stocker Road, Exeter, EX4 4PB, UK,

+44 1392 723495, E-mail *Andrew.m.shaw@exeter.ac.uk*

Classification: Biological Sciences; Systems Biology

Abstract

Recombinant protein A/G (PAG) has a sequence coding for eight IgG binding sites and has enhanced inter-species affinity. High-frequency sampling of a PAG titration with IgG produces concentration profiles that are sensitive to the kinetic availability of the binding sites. The full kinetic model developed here for IgG binding sequentially to PAG shows only two distinct kinetic processes, describing an initial rapid association of two antibodies to PAG with a rate constant k-fast = 1.86 ± 0.08 × 10^6 M^{-1} s^{-1} and a slower antibody binding process to all remaining sites, k-slow = 1.24 ± 0.05 × 10^4 M^{-1} s^{-1}. At equilibrium (after 1 hour), the maximum IgG occupancy of PAG is 2.8 ± 0.5, conflicting with the genetic evidence of eight binding sites and suggesting significant steric hindrance of the neighbouring IgG binding sites. The phosphate-buffered saline (PBS) solution defines a standard System Setting and this may be compared with other settings. The mean association rate of PAG-IgG_n in the standard setting is 282 ± 20% higher than when PAG is tethered to a surface. A systems biology approach requires that a model parameter set that define a system in a Standard Setting should be transferable to another system. The transfer of parameters between settings may be performed using activity coefficients characterising an effective concentration of species in a system, $a_i = \gamma_i c_i$. The activity correction, γ for the 8-site occupancy is $\gamma = 0.35 \pm 0.06$ and mapping from the standard setting to solution setting suggests $\gamma_{PAG-IgG} = 0.4 \pm 0.03$. The role of activity coefficients and transferability of kinetic parameters between system settings is discussed.

Introduction

Multivalent protein-ligand binding is a fundamental biochemical interaction that is of interest for both native proteins in their typical environments as well as modified proteins with tailored applications. The genetically-modified protein A/G (PAG) has eight binding sites optimised with high specificity to mammalian immunoglobulins by combining the IgG binding domain sequences of Staphylococcal protein A (SPA) and Streptococcal protein G (SPG): a model multivalent binding system, PAG-IgG_n [1 2]. The PAG-IgG_n model is characterised by data from many sources starting with the genetic sequence from which there is "genetic evidence" of 8 binding sites with a well-characterised structure and affinity for IgG[2]. The Fc binding domains of SPA and SPG have been used as a proxy for FcγR receptors on the surface of phagocytes[3-4] and the binding domain crystal structures have been solved.[5-6] PAG is widely used for ligand capture in affinity chromatography[7] where there is a tacit assumption that the protein activity on a separation surface is the same as in solution and in large excess due to the number of binding sites and mass on the surface. However, when purchased, PAG is described as having 6 binding sites, despite the genetic evidence and there is clearly an unknown fraction of binding sites available sterically, Figure 1.

There is a particularly strong link between genetic modification and kinetic mechanism in the field of synthetic multivalent ligand binding in next-generation therapeutic agents and biomaterials.[8] The architecture of synthetic protein scaffolds may be genetically designed to vary size and valency, which control reaction kinetics and mechanism of action.[9] Careful quantitative characterisation however, requires a suitable sampling frequency to establish kinetically distinct mechanisms from which a set of uncoupled kinetic parameters may be derived. The goal of Systems Biology in fields such as personalised medicine[10] is to combine data from all sources such as *in vivo* and *in vitro* measurements, genetic sequence information and surface sensor measurements, to produce a model that is predictive in different system settings (healthy and sick patient serum for example). The quantitative mechanism must start with the rate of a second order reaction in a model, which is written:

$$Rate = k_{12}\,[c_1][c_2] \qquad (1)$$

where $[c_1]$ and $[c_2]$ are the reactant concentrations and k_{12} is the second order rate constant. This equation may describe the reaction in a standard system setting such as phosphate-buffered saline (PBS). The active or effective concentration of a species available in a different system setting may be treated in as the product of the activity coefficient and the measured concentration and is written:

$$a_1 = \gamma_1[c_1] \quad (2)$$

where γ_1 is the effective activity coefficient of the species c_1. The effective activity of a species depends on the difference in the observed system setting (cytoplasm or serum for example), from the standard setting in PBS. Significant differences in the effective activity of a species observed in varying system settings may fundamentally limit the predictive usefulness of a deterministic model derived from a single setting.[11] These transferability uncertainties of γ_i capture the difficulty in moving between system settings and may go some way to explain observations of enzymes apparently beating the diffusion limit for chemical reactions,[12] where γ would be greater than 1.

The fully predictive kinetic model is burdened by familiar challenges such as measuring data that are sensitive to kinetically distinct processes, uncertainties in the determining the global minimum during model optimisation and subsequent high correlation between model parameters. Parameters may become model-dependent or system-setting dependent and properties such as affinity and avidity with unknown steric effects and interface activity[13] [14] likely differ between system settings. There are some notable exceptions such as isothermal calorimetry and stopped-flow fluorescence studies, which exemplify a good agreement of solution and interface studies with approximately 5% error[15] in specific cases. However, system-invariant parameters will need to be established for each new system setting individually. Even thorough tests of model parameter purity, starting point invariance and high confidence in the global fit solution[16] cannot reduce the uncertainty in the activity of proteins and variation of kinetic parameters in untested system settings.

In this paper, we present a series of experiments rapidly sampling the association kinetics of IgG to recombinant PAG to detect multiple ligand binding events and use all available evidence to construct a fully quantitative kinetic analysis of the of multi-ligand binding interactions. A deterministic model is constructed for 8 binding sites (as indicated by the genetic evidence) from which a set of rate constants and activity coefficients are derived in the standard system setting of PBS. Multiple parameter search methods are considered to fit the data and dimensionality reduction of the model is performed, based on a parameter correlation analysis. The reaction kinetics in the standard system setting are compared to those in an alternate system setting where PAG is immobilised on a sensor surface, from which further kinetic parameters are derived with activity coefficients. The role of PBS as a Standard System Setting, analogous to the standard conditions of thermodynamics, is considered together with the transferability of kinetic parameters using the concept of activity coefficients.

Materials and Methods

Pierce recombinant protein A/G (5 mg) was obtained from Thermo Scientific (#21186). IgG antibody used was Rabbit anti-Sheep (1 mg/mL) obtained from Bio-Rad (#5184-2304). Human serum albumin and bovine serum albumin were obtained from Sigma-Aldrich. Standard instrument running buffer, also used in preparation and dilution of the samples, was phosphate-buffered saline (PBS) supplied in tablet form by Sigma-Aldrich. Ortho-phosphoric acid (85%) was obtained from Fluka and a 0.1 M aqueous solution used as regeneration buffer. GAPSII aminated glass prep slides were obtained from Corning (#40006).

The binding kinetics of IgG binding to surface tethered PAG were determined using a biophotonic multiplexed detection platform described in detail elsewhere.[17] Briefly, a gold seed nanoparticle array is printed with inkjet printer onto a surface and grown into highly sensitive light scatter centres. The array is returned to the printer for assay functionalisation with an antigen for specific antibody detection, an antibody for antigen detection, or protein A/G for total a total IgG assay. The biophotonic array is illuminated in total-internal reflection and scattered light is captured by video camera normal to the array surface and at the video-frame rate, to produce the immune-kinetic trace, Figure S1. The IgG test array was constructed using 24 assay elements functionalised with PAG printed from a 2 mg/mL solution in PBS and 50% glycerol; 16 light intensity controls were printed from a 2 mg/mL solution of BSA in PBS for reproducibility. The control elements are used to remove the effect of refractive index variation with temperature, intensity changes in the lamp illumination and non-specific protein binding. Nonspecific binding sites on the array surface are blocked with human serum albumin (5 μM, 300 seconds) before assay operation.

Standard solutions of IgG (2.5 nM, 25 nM, 50 nM, 100 nM, 200 nM) are injected over the assay surface for a fixed period of 100 seconds to monitor association kinetics to PAG and washed in PBS for 200s to monitor dissociation kinetics. Association and dissociation timescales were chosen to provide typical errors in estimated association and dissociation rate constants of <15% and <10% respectively,[3] whilst allowing rapid sampling of 5 minutes per sample. The immune-kinetic assay traces, Figure S1, are fitted simultaneously for all concentrations to a simple 1:1 Langmuirian adsorption isotherm model to produce a global fit.[3] The kinetic model of the interface of the sensor surface produces average estimates for k_a and k_d: $3.26\pm0.03\times10^5$ M^{-1} s^{-1} and $3.01\pm0.37\times10^{-4}$ s^{-1} respectively, which compare favourably with literature values [18].

The IgG immune-kinetic assay is calibrated using the area-under-the-curve of the association step, plotted against IgG concentration and fitted to a 4-parameter logistic (Figure S1) with a resulting R^2 of 0.997. The IgG assay Limit of Detection (3σ of the noise distribution of the PBS blank) is 4.7×10^{-5} RIU

corresponding to 0.4 nM. The Limit of Quantitation, (10σ of the noise distribution of the PBS blank) is 1.7 nM. The typical assay error, estimated from 9 sample repeats at 100 nM, is 5 nM (2σ, 95% confidence limit). The sampling frequency for the IgG assay is every 5 minutes, allowing for a surface regeneration step after each sample measurement, which removes captured IgG in preparation for the next sample.

PAG-IgG reaction mixtures are prepared with PAG mole fractions of: 0.09, 0.14, 0.2, 0.25, 0.3, 0.35, 0.43 and 0.5. The starting IgG concentration is 100 nM for each mole fraction. The IgG concentration in a 500 µL sample of each reaction mixture is measured at 50±30s after mixing and every 5 minutes thereafter for 1 hour.

Results and Discussion

The effective activity of the recombinant-antibody-binding protein, PAG, was studied quantitatively, label-free in solution and modelled using a deterministic ordinary differential equation model fitting to the experimental data – a classic systems biology approach. Binary solutions of IgG/PAG were prepared with different PAG mole fractions (*x*PAG) in the range 0 – 0.5 (corresponding to starting ratios in the range 1:0 to 1:1 IgG:PAG). The solutions were sampled for unbound IgG within 50 seconds of mixing and sampled every 5 minutes for 1 hour, using an immuno-kinetic assay with a limit of quantitation of 1.7 nM, Figure 2. From an initial IgG concentration of 100 nM, the antibody concentration is seen to fall rapidly within the first 50 seconds followed by further, slower decrease over the next hour. The decrease in total IgG in solution after the first 50 seconds is shown in Figure 2(b) and has a zero asymptote (LoQ 1.7 nM) at mole fractions of PAG in the range 0.35 - 0.43, corresponding to 1.6 ± 0.3 IgG molecules bound to PAG. The effective activity of PAG during the initial 50 seconds of association is the ratio of bound IgG to the genomic maximum of 8 sites[2], $\gamma_{PAG} = \frac{1.6 \pm 0.3}{8} = 0.20 \pm 0.04$. The apparent cooperative binding effect observed in Figure 2(b) has been previously reported for SPA[19] and may be explained by fewer antibodies bridging two PAG proteins by binding to two sites at higher mole fractions of antibody.[20]

The number of bound IgG per individual PAG after 1 hour, Figure 3, is 2.8 ± 0.5, markedly similar to the literature values for SPA (2.5 - 3.1) [21] and corresponding to a $\gamma_{PAG} = \frac{2.8 \pm 0.5}{8} = 0.35 \pm 0.06$. The stoichiometry of PAG-IgG binding interaction after 1 hour is significantly below the 8 binding sites suggested by the sequence[2] or the 6 binding sites as sold by many suppliers. The steric blocking of neighbouring IgG binding sites on the genetically modified PAG appears to be no better than for native SPA. Despite reports that the sum of weaker contacts in a flexible context around a central scaffold can be more efficient than precise design and strong individual interactions[22], steric hindrance

between binding domains must be considered in ligand design. Future synthetic Fc binding proteins should include contacts around platforms with considered geometries able to better accommodate IgG in all binding sites.

An ordinary differential equation (ODE) model is presented here for the sequential filling of 8 binding sites (the number suggested by the genetics literature) on the PAG molecule assuming sequential non-cooperative binding. The model is described by molecular equations 1a-8a and mathematically by differential equations 1b-8b with k_a and k_d representing the forward and reverse reaction rate constants respectively. All effective activity coefficients are assumed to be 1.

$$IgG + PAG \underset{k_{d1}}{\overset{k_{a1}}{\rightleftarrows}} IgG_1PAG \quad (1a) \qquad \frac{d[IgG]}{dt} = k_{d1}[IgG_1PAG] - k_{a1}[IgG][PAG] \quad (1b)$$

$$IgG + IgG_1PAG \underset{k_{d2}}{\overset{k_{a2}}{\rightleftarrows}} IgG_2PAG \quad (2a) \qquad \frac{d[IgG]}{dt} = k_{d2}[IgG_2PAG] - k_{a2}[IgG][IgG_1PAG] \quad (2b)$$

$$IgG + IgG_2PAG \underset{k_{d3}}{\overset{k_{a3}}{\rightleftarrows}} IgG_3PAG \quad (3a) \qquad \frac{d[IgG]}{dt} = k_{d3}[IgG_3PAG] - k_{a3}[IgG][IgG_2PAG] \quad (3b)$$

$$IgG + IgG_3PAG \underset{k_{d4}}{\overset{k_{a4}}{\rightleftarrows}} IgG_4PAG \quad (4a) \qquad \frac{d[IgG]}{dt} = k_{d4}[IgG_4PAG] - k_{a4}[IgG][IgG_3PAG] \quad (4b)$$

$$IgG + IgG_4PAG \underset{k_{d5}}{\overset{k_{a5}}{\rightleftarrows}} IgG_5PAG \quad (5a) \qquad \frac{d[IgG]}{dt} = k_{d5}[IgG_5PAG] - k_{a5}[IgG][IgG_4PAG] \quad (5b)$$

$$IgG + IgG_5PAG \underset{k_{d6}}{\overset{k_{a6}}{\rightleftarrows}} IgG_6PAG \quad (6a) \qquad \frac{d[IgG]}{dt} = k_{d6}[IgG_6PAG] - k_{a6}[IgG][IgG_5PAG] \quad (6b)$$

$$IgG + IgG_6PAG \underset{k_{d7}}{\overset{k_{a7}}{\rightleftarrows}} IgG_7PAG \quad (7a) \qquad \frac{d[IgG]}{dt} = k_{d7}[IgG_7PAG] - k_{a7}[IgG][IgG_6PAG] \quad (7b)$$

$$IgG + IgG_7PAG \underset{k_{d8}}{\overset{k_{a8}}{\rightleftarrows}} IgG_8PAG \quad (8a) \qquad \frac{d[IgG]}{dt} = k_{d8}[IgG_8PAG] - k_{a8}[IgG][IgG_7PAG] \quad (8b)$$

The ODE solutions are propagated numerically (Runge-Kutta) and fitted simultaneously to all of the data in Figure 2, with equal weighting, using a non-linear least squares trust region reflective method[23-24]. All data processing is performed off-line using a commercial software package (MATLAB R2016a). The initial guess values for the association and dissociation rate constants of the fitting routine are taken from the interface biosensor study, fitting all of the association and dissociation traces, Figure S1, simultaneously. The model fit does not converge when all 16 rate constants are allowed to change, owing to the high correlations between the parameters and multiply degenerate solutions for all positions in parameter space.

The first parameter reduction technique is to fix the PAG-IgG dissociation rate at the rate observed on the surface. The dissociation rate or complex half-life reflects how well bound the IgG is to the PAG which is least likely to vary between settings. There is little opportunity for surface avidity for the Fc region binding and constant complex half-life is a reasonable assumption. The dissociation rates for all PAG-IgG_n complexes are set at $3.01 \times 10^{-4}\ s^{-1}$ and the association rates of all reactions are fitted to the data. The 8 association rate constants are determined with poor confidence (Table S1) and remain highly correlated; the correlation matrix can be seen graphically in Figure 4 and numerically in Table S2. The heat map of the correlation matrix, Figure 4a shows a striking division into two parameter regimes and the correlation graph in figure 4b shows the connectivity of the rate constants. The parameters in the model may be grouped based on the correlation connectivity into a single fast association reaction, combining k_{a1} - k_{a2}, and k_{a3}-k_{a8} into a single slow-kinetic association, allowing the fit to converge with good root-mean-square-error (RMSE), improved parameter confidence and reduced parameter correlation,

Table 1.

The 8-binding site ODE model may also be reduced to sequential filling of 3 binding sites only (the number determined experimentally by titration, Figure 3) using the same parameter grouping as the 8-site model (*k*-fast = $k_{a1\text{-}2}$ and *k*-slow = k_{a3}). The RMSE for the 8 site and 3 site models are not significantly different; 3.25 nM and 3.31 nM respectively. Considering both goodness-of-fit and titration data, the reaction mechanism in solution is best described by 3 antibody binding steps, rather than 8 as predicted by the genetic evidence. The correlation coefficient between *k*-fast and *k*-slow, is -0.030 and -0.052 for both models respectively, indicating that the *k*-fast and *k*-slow parameter groups are kinetically distinct in the data.

There are two observations with consequences for spin-column separation science: the surface excess of binding sites for PAG on the surface may be significantly lower than expected and loading times for the column may be as short as 50 seconds rather than 10 minutes as indicated in some protocols. Both binding site models have the same fitted *k*-fast rate constant and predict that after 50 seconds, unbound IgG concentration is reduced by 50% and 99% at PAG mole fractions of 0.20 and 0.43 respectively (Figure 2). The antibody titration shows that $k_{a1\text{-}2}$ dominate the reaction in early time and complete antibody binding may be achieved rapidly with sufficient excess of PAG of antibody. Over-loading of the column is probably the major concern if reliance on 6-fold binding site excess (as sold) or 8-fold as indicted genetically were critical in the adoption or modification of a protocol.

Two systems settings may now be compared with the activity formalism: solution and interface. The association rate of the IgG-PAG reaction differs significantly between solution and surface tethered PAG (

Table 1). The fitted 8-site and 3-site models have mean association rate constants that are 47 ± 8 % and 282 ± 20 % greater than k_a derived from biosensor data of the IgG association to tethered PAG at a plasmon surface (3.26 ± 0.03 ×10^5 M^{-1} s^{-1}). The difference between the interface and solution-phase reaction rates may be attributed to several factors including differences in diffusion coefficients (limiting rate constants), reduced effective activity at the interface and limited transport across any interface that forms between the tethered proteins and the bulk solution. However, there is also a clear steric effect with the acceptance angle of the surface collision (Figure 1) likely limited to a solid angle of ~2π steradians with consequences for surface packing[20], enhanced co-operative binding[19] and potentially different surface complexes including surface avidity[25] and bridging. These latter effects are apparent as departures from the 1:1 surface binding model that are visible in the multi-concentration global fit to the 1:1 binding kinetics (Figure S1). All these effects can be grouped into 'effective activity' that would show concentration dependence, leaving a "pure" transferable rate constant that could be determined under conditions of low surface protein density and low solution IgG concentrations to provide a best estimate of the limiting value for the rate constant and hence the thermodynamics of the complex stability.

The *k*-fast and *k*-slow rate constants reduction demonstrates a persistent challenge for systems biology and more generally kinetics. Kinetically distinct processes in a deterministic model must have significantly different rates to be determined experimentally, highlighting that kinetic data need to be recorded at a sufficiently rapid sampling rate. Similar fast or slow kinetic processes may never be distinguishable. Secondly, even with high quality data, there must be a global minimum in the fitted model if the kinetic parameters are to decouple sufficiently to allow the model to be predictive. The *k*-fast-*k*-slow parameter space in the current model can be explored in a box search and plotted in 3D with RMSE as the figure of merit of the fit, Figure 5. The parameter space exploration allows the depth of the global minimum from the starting point is 27.0 – 3.46 nM (RMSE) for the 8-site model and 12.6 – 3.31 nM (RMSE) for the 3-site model. Critically, two fitting routines, least squares and a pattern search method[26], find the same minimum and show good starting-point invariance. Starting point invariance is a good test of model accuracy but is rarely checked so easily. There can be reasonable certainty in the purity of the two grouped rate constants k-fast and k-slow and that their resolution into kinetically distinct process is constrained by the lack of data in the first 50 seconds. Hence with

some confidence, the PAG-$IgG_{1\text{-}3}$ interaction is accurately described by two processes: an initial rapid binding of two IgG ligands followed more slowly by at most one further IgG.

The concept of a standard setting must be considered. For protein-protein interactions the standard setting must capture the fundamental kinetics and thermodynamics of the interaction minimising the effects of concentration perturbations such as hydrodynamic effects in the crowded environments of cell cytoplasm[27]. The rate constants determined in the standard setting provide the best understanding of association, dissociation and affinity of the ligand-protein interaction and define the standard number of binding sites. PAG-IgG does not have 8-sites as predicted by the genetic sequence. In the cytoplasm, as much as 40% of the total volume may be occupied by proteins, and crowding effects will generate several perturbations to protein-protein interactions and ligand binding. Reduced diffusion rate also changes the collision number within the environment. Interactions may be sterically favoured or hindered and concentrations of reactants may be enhanced or depleted by association with different components. The description of the second order reaction in equation (1) with the activity, γ_i, in equation (2) captures the variations between the simple system settings observed. One approach is to fix the concentration and reaction rate constant at the standard system setting, PBS, which captures the kinetics and thermodynamics of the ligand-binding site interactions and introduce an activity coefficient, γ_i, that needs to be well defined for the standard setting. In this study, the number of kinetically active sites, $\gamma_{PAG} = \frac{2.8 \pm 0.5}{8} = 0.35 \pm 0.06$, defines an effective activity for the PAG in PBS. Parameter transfer between system settings requires the contributing factors to be identified and trends in increasing molecular crowding to be understood or measured empirically.

Conclusions

The transferability of parameters from one set of fitted data to any new system setting is required if a systems biology model is to be usefully predictive. A clear starting point of a standard setting in PBS is capturing the kinetics and thermodynamics of the protein-ligand binding interactions in standard conditions. Transition to other system settings modifies the protein concentrations with an activity coefficient, γ_1, and fundamentally the interactions themselves but identifies considerable variations. The binding capacity of the PAG-IgG interaction is a maximum of 2.8 ± 0.5 IgG in solution despite genomic evidence suggesting the availability of 8 binding sites. The activity coefficient for binding is $\gamma_{PAG} = 0.35 \pm 0.06$. Similarly, interface and solution rate parameters for the PAG-IgG ligand binding interaction are observed to be significantly different and consequently PAG-IgG activity at the interface may be defined as $\gamma_{PAG-IgG} = 0.40 \pm 0.03$, based on the estimates of the rate constants

of the 3-binding site model in solution. The different contributions from γ_{PAG} and γ_{IgG} to the standard system binding model presented here are unknown and understanding the product of effective activity and rate constants may be a fundamental uncertainty of systems biology. Hence models of the immune system for instance may change for a healthy patient to a sick patient where the patient's response changes the viscosity and protein composition of the serum. Amplification of transferability uncertainties through a larger reaction networks in a more complex system would likely lead to a loss of any model predictability. Model parameters derived from genomics or from alternate systems settings should be used with caution when developing systems biology models and may not be transferrable.

Acknowledgements

Funding Sources: EPSRC Studentship in collaboration with The University of Exeter Medical School.

Supporting Information Available

Figure S1 shows immune-kinetic assay data from which the protein A/G – IgG binding kinetics were derived in the 'surface setting' and a standard curve using the area under the curve was obtained. The standard curve is used to quantify unbound IgG during the same reaction in the 'solution setting'. Table S1 shows the parameter estimates from the 8-binding site fit where each association rate constant is allowed to float. Confidence intervals are shown as a percentage of the estimate. Table S2 is the correlation matrix from the 8-binding site fit. This information is available free of charge via the Internet at http://pubs.acs.org

Figures and Tables

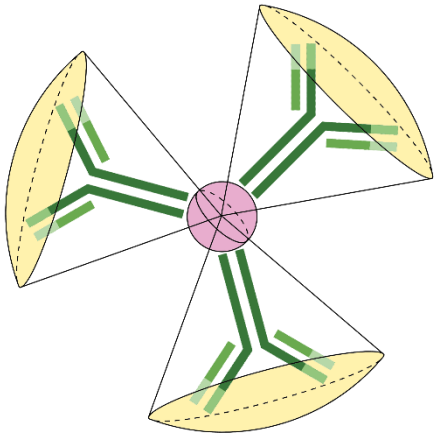

Figure 1 Protein A/G (purple) binding to IgG (green). Each bound IgG will occupy a fraction of the available spherical surface area (yellow) and must reduce the solid angle available to further IgG molecules.

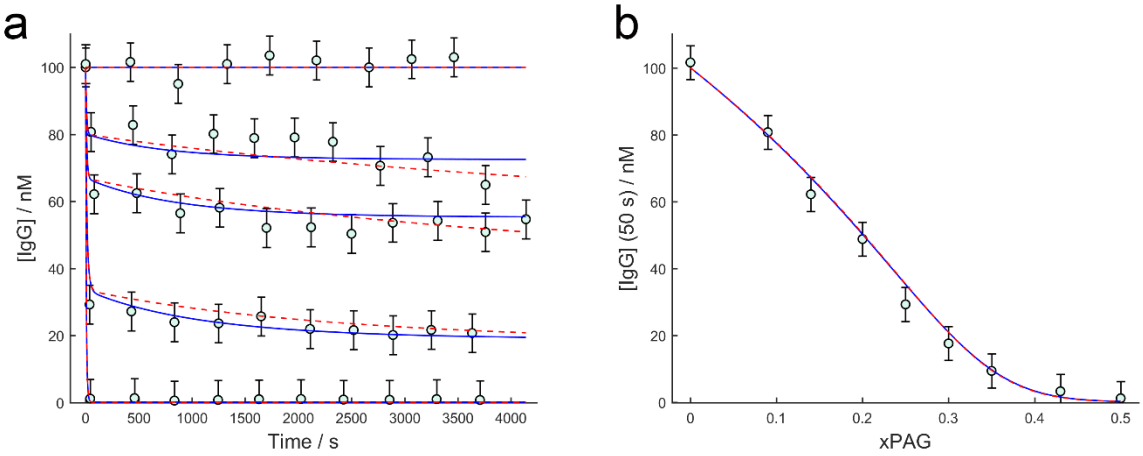

Figure 2 Time course analysis of IgG binding to solution phase recombinant protein A/G. a) Unbound IgG concentration is shown for varying ratios of antibody and PAG: control, 10:1, 6:1, 3:1, 1:1. Error bars are ±2σ typical assay error, 5nM. The data are fit to a kinetically distinct 3-binding site model (solid blue) and an 8-binding site model (dashed red). b) Titration of the free IgG against the mole fraction of Protein A/G, sampled at the end of the first kinetic process 50±30 seconds after mixing. Error bars are ±2σ typical assay error, 5nM. A 3-site model (solid blue) and an 8-site model (dashed red) are overlaid.

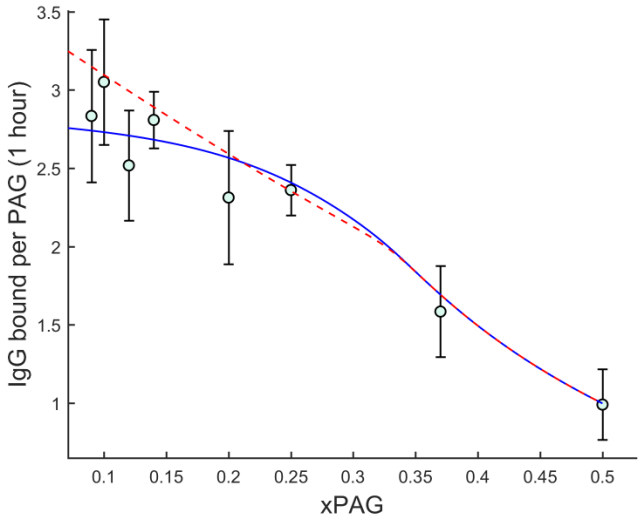

Figure 3 Effective stoichiometry of antibody (IgG) bound per protein A/G binding at varying mole fractions of protein A/G. Data are derived from the mean of triplicate IgG samples at 55 minutes ±5 minutes after mixing with protein A/G; error bars are ±2σ. A 3-binding site model (solid blue) and an 8-binding site model (dashed red) are overlaid.

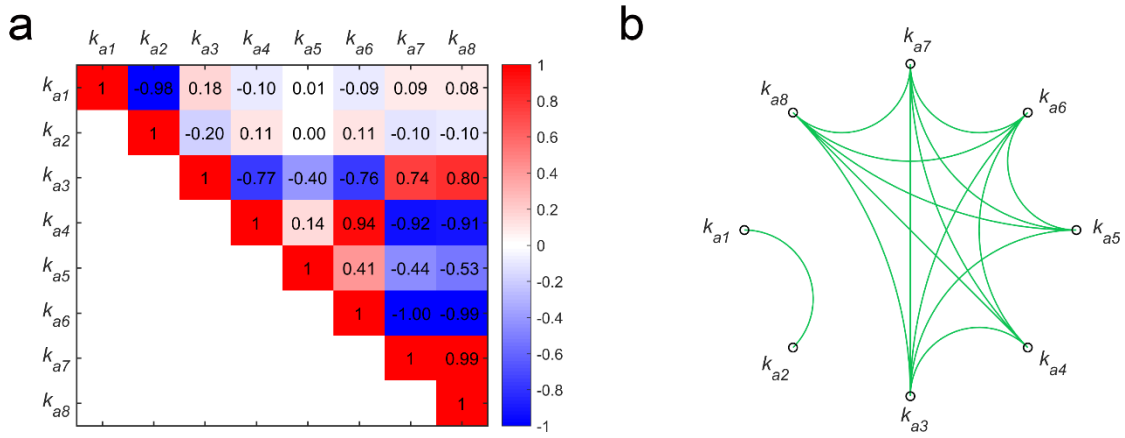

Figure 4 Parameter correlation for the 8 binding site, 8-parameter fit of the association rate constant parameters only. The initial guess values for the association rate constants of the fitting routine were taken from the interface biosensor study. a) Heat map of the correlation matrix, b) Node map of absolute pairwise parameter correlation, showing two distinct groups of parameters. Every model parameter is represented by a node and is linked to another parameter node if their absolute pairwise correlation is greater than 0.2. The figure highlights the rationale for grouping $k_{1\text{-}2}$ into k-fast and $k_{3\text{-}8}$ into k-slow.

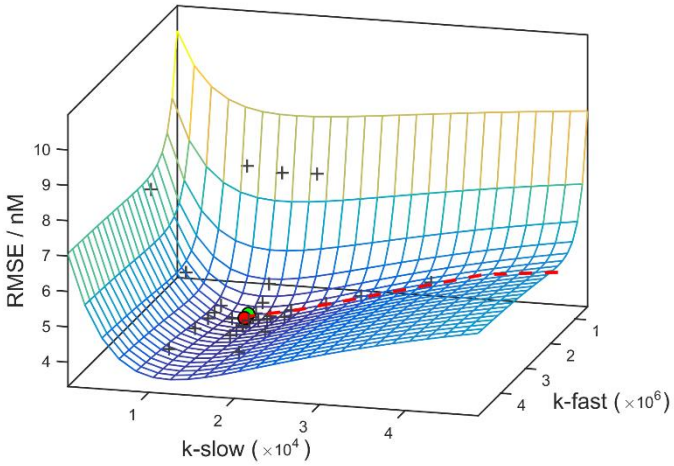

Figure 5 Box-search parameter space of root mean square error at various combinations of k-fast and k-slow for the 3-binding site fit. The global minimum estimated by pattern search (green sphere) is within 95% confidence limits of the least squares fit result (red sphere). The least squares fit search path (red dashed line) and pattern search points (black crosses) originate from k-fast and k-slow initial guesses set at the surface studies value of 3.26×10^5 (outside plot range).

	Fit Property	Biosensor Interface Value	Least squares local minimum estimate	Pattern search global minimum estimate
8 binding site model	*k*-fast / M^{-1} s^{-1}	3.26×10^5	$1.90 \pm 0.09 \times 10^6$	1.89×10^6
	k-slow / M^{-1} s^{-1}	3.26×10^5	$6.10 \pm 0.01 \times 10^3$	6.10×10^3
	k_d / s^{-1}	3.01×10^{-4}	-	-
	RMSE / nM	27.0	3.46	3.46
3 binding site model	*k*-fast / M^{-1} s^{-1}	3.26×10^5	$1.86 \pm 0.08 \times 10^6$	1.85×10^6
	k-slow / M^{-1} s^{-1}	3.26×10^5	$1.24 \pm 0.05 \times 10^4$	1.24×10^4
	k_d / s^{-1}	3.01×10^{-4}	-	-
	RMSE / nM	12.6	3.31	3.31

Table 1 Results of fitting 8 and 3 binding site models to IgG-PAG binding time course data

References

1. Eliasson, M.; Andersson, R.; Olsson, A.; Wigzell, H.; Uhlén, M. Differential IgG-binding characteristics of staphylococcal protein A, streptococcal protein G, and a chimeric protein AG. *J. Immunol.* **1989,** *142*, 575-81.
2. Eliasson, M.; Olsson, A.; Palmcrantz, E.; Wiberg, K.; Inganäs, M.; Guss, B.; Lindberg, M.; Uhlén, M. Chimeric IgG-binding receptors engineered from staphylococcal protein A and streptococcal protein G. *J. Biol. Chem.* **1988,** *263*, 4323-4327.
3. Read, T.; Olkhov, R. V.; Williamson, E. D.; Shaw, A. M. Label-free Fab and Fc affinity/avidity profiling of the antibody complex half-life for polyclonal and monoclonal efficacy screening. *Anal. Bioanal. Chem.* **2015,** *407*, 7349-7357.
4. Sondermann, P.; Huber, R.; Oosthuizen, V.; Jacob, U. The 3.2-Å crystal structure of the human IgG1 Fc fragment-FcγRIII complex. *Nature* **2000,** *406*, 267-273.
5. Deisenhofer, J. Crystallographic refinement and atomic models of a human Fc fragment and its complex with fragment B of protein A from Staphylococcus aureus at 2.9- and 2.8- Å. resolution. *Biochemistry* **1981,** *20*, 2361-2370.
6. Sauer-Eriksson, A. E.; Kleywegt, G. J.; Uhlén, M.; Jones, T. A. Crystal structure of the C2 fragment of streptococcal protein G in complex with the Fc domain of human IgG. *Structure* **1995,** *3*, 265-278.
7. Huse, K.; Böhme, H.-J.; Scholz, G. H. Purification of antibodies by affinity chromatography. *J. Biochem. Biophys. Methods* **2002,** *51*, 217-231.
8. Kiessling, L. L.; Strong, L. E.; Gestwicki, J. E. Principles for multivalent ligand design. *Annu. Rep. Med. Chem.*, Academic Press: 2000; 35, pp 321-330.
9. Kiessling, L. L.; Gestwicki, J. E.; Strong, L. E. Synthetic Multivalent Ligands as Probes of Signal Transduction. *Angew. Chem. Int. Edit* **2006,** *45*, 2348-2368.
10. Hood, L.; Heath, J. R.; Phelps, M. E.; Lin, B. Systems Biology and New Technologies Enable Predictive and Preventative Medicine. *Science* **2004,** *306*, 640-643.
11. Kirk, P. D. W.; Babtie, A. C.; Stumpf, M. P. H. Systems biology (un)certainties. *Science* **2015,** *350*, 386-388.
12. Bar-Even, A.; Noor, E.; Savir, Y.; Liebermeister, W.; Davidi, D.; Tawfik, D. S.; Milo, R. The Moderately Efficient Enzyme: Evolutionary and Physicochemical Trends Shaping Enzyme Parameters. *Biochemistry* **2011,** *50*, 4402-4410.
13. De Crescenzo, G.; Pham, P. L.; Durocher, Y.; O'Connor-McCourt, M. D. Transforming Growth Factor-beta (TGF-β) Binding to the Extracellular Domain of the Type II TGF-β Receptor: Receptor Capture on a Biosensor Surface Using a New Coiled-coil Capture System Demonstrates that Avidity Contributes Significantly to High Affinity Binding. *J. Mol. Biol.* **2003,** *328*, 1173-1183.
14. Fan, X.; White, I. M.; Shopova, S. I.; Zhu, H.; Suter, J. D.; Sun, Y. Sensitive optical biosensors for unlabeled targets: A review. *Anal. Chim. Acta* **2008,** *620*, 8-26.
15. Day, Y. S. N.; Baird, C. L.; Rich, R. L.; Myszka, D. G. Direct comparison of binding equilibrium, thermodynamic, and rate constants determined by surface- and solution-based biophysical methods. *Protein Sci.* **2002,** *11*, 1017-1025.
16. Sigmundsson, K.; Másson, G.; Rice, R.; Beauchemin, N.; Öbrink, B. Determination of Active Concentrations and Association and Dissociation Rate Constants of Interacting Biomolecules: An Analytical Solution to the Theory for Kinetic and Mass Transport Limitations in Biosensor Technology and Its Experimental Verification. *Biochemistry* **2002,** *41*, 8263-8276.
17. Olkhov, R. V.; Fowke, J. D.; Shaw, A. M. Whole serum BSA antibody screening using a label-free biophotonic nanoparticle array. *Anal. Biochem.* **2009,** *385*, 234-241.
18. Bronner, V., Tabul, M. and Bravman, T. Protein interaction analysis tech note 5820: rapid screening and selection of optimal antibody capturing system. http://www.bio-rad.com/webroot/web/pdf/lsr/literature/Bulletin_5820A.pdf (accessed 16/12/2016).
19. O'Keefe, E.; Vennett, V. Use of immunoglobulin-loaded protein A-bearing staphylococci as a primary solid phase immunoadsorbent in radioimmunoassay. *J. Biol. Chem.* **1980,** *255*, 561-568.

20. Hanson, D. C.; Schumaker, V. N. A model for the formation and interconversion of protein A-immunoglobulin G soluble complexes. *J. Immunol.* **1984,** *132*, 1397-409.
21. Ghose, S.; Hubbard, B.; Cramer, S. M. Binding capacity differences for antibodies and Fc-fusion proteins on protein A chromatographic materials. *Biotechnol. Bioeng.* **2007,** *96*, 768-779.
22. Martos, V.; Castreño, P.; Valero, J.; de Mendoza, J. Binding to protein surfaces by supramolecular multivalent scaffolds. *Curr. Opin. Chem. Biol.* **2008,** *12*, 698-706.
23. Coleman, T. F.; Li, Y. An Interior Trust Region Approach for Nonlinear Minimization Subject to Bounds. *SIAM J. Optim.* **1996,** *6*, 418-445.
24. Coleman, T. F.; Li, Y. On the convergence of interior-reflective Newton methods for nonlinear minimization subject to bounds. *Math. Prog.* **1994,** *67*, 189-224.
25. Ogi, H.; Motohisa, K.; Hatanaka, K.; Ohmori, T.; Hirao, M.; Nishiyama, M. Concentration dependence of IgG–protein A affinity studied by wireless-electrodeless QCM. *Biosens. Bioelectron.* **2007,** *22*, 3238-3242.
26. Kolda, T. G.; Lewis, R. M.; Torczon, V. A generating set direct search augmented Lagrangian algorithm for optimization with a combination of general and linear constraints. *Sandia National Laboratories* **2006,** *6*.
27. Ando, T.; Skolnick, J., Crowding and hydrodynamic interactions likely dominate in vivo macromolecular motion. *Proc. Natl. Acad. Sci.* **2010,** *107*, 18457-18462.

For Table of Contents Use Only

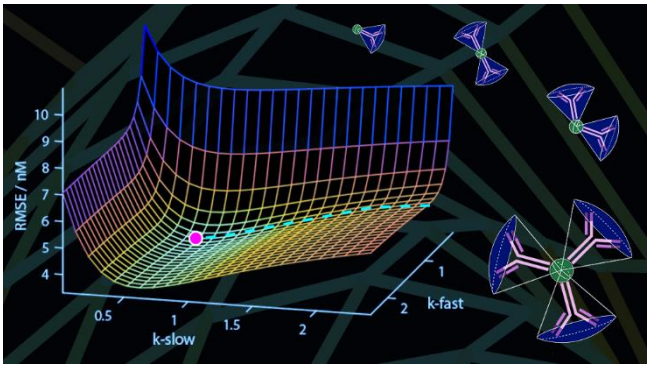

TOC Graphic